S-wave heavy quarkonium spectrum with next-to-next-to-next-to-leading logarithmic accuracy

Daniel Moreno Torres

Institut de Física d'Altes Energies (IFAE)
Universitat Autònoma de Barcelona (UAB)
Spain

QWG 2019 - The 13th International Workshop on Heavy Quarkonium
May 14, 2019

Outline

Introduction

High order perturbative computations in heavy quarkonium require the use of effective field theories (EFTs), as they facilitate the systematic resummation of the large logarithms generated by the ratios of the different scales of the problem.

Integrating out larger scales we derive pNRQCD[1], a theory optimised to the description of heavy quarkonium near threshold:

QCD

$\downarrow$ Integrating out the hard scale m
(heavy quark mass)

NRQCD

$\downarrow$ Integrating out the soft scale mv
(inverse Bohr radius)

pNRQCD

d.o.f with ultrasoft energy $E \sim mv^2$
(typical binding energy)

[1] A. Pineda, and J. Soto, Nucl. Phys. Proc. Suppl. **64**, 428 (1998) and N. Brambilla, A. Pineda, J. Soto, and A. Vairo, Nucl. Phys. **B566**, 275 (2000).

Introduction

At present, the pNRQCD Lagrangian is known

- With N^{3}LO accuracy[2].
- With N^{3}LL precision for P-wave ($l \neq 0$) states[3].
- With N^{2}LL precision for S-wave ($l = 0$) states[4].

The missing link to obtain the complete N^{3}LL pNRQCD Lagrangian is the N^{3}LL running of the delta-like potentials[5]

- For the spin-dependent (SD) case already achieved[6]
- For the spin-independent (SI) case MISSING!

[2] B. A. Kniehl, A. A. Penin, V. A. Smirnov, and M. Steinhauser, Nucl. Phys. **B635**, 357 (2002); C. Peset, A. Pineda, and M. Stahlhofen, J. High Energy Phys. 05, (2016) 017.

[3] C. Peset, A. Pineda, and J. Segovia, Phys. Rev. D **98**, 094003 (2018)

[4] A. Pineda, Phys. Rev. D **65**, 074007 (2002)

[5] We use the term "delta-like potentials" for the delta potential and the potentials generated by the Fourier transform of $\ln^n k$ (in practice only $\ln k$).

[6] B. A. Kniehl, A. A. Penin, A. Pineda, V. A. Smirnov, and M. Steinhauser, Phys. Rev. Lett. **92**, 242001 (2004); **104**, 199901(E) (2010); A. A. Penin, A. Pineda, V. A. Smirnov, and M. Steinhauser, Phys. Lett. B **593**, 124 (2004); **677**, 343(E) (2009). Be careful when comparing with ours, as there is a change in the basis of potentials.

Introduction

Aim: Determine the SI delta-like potential with N^{3}LL accuracy (or its associated Wilson coefficient $\tilde{D}_d^{(2)}$ with NLL accuracy)

$\Rightarrow$ Necessary precision to obtain the S-wave spin-average energy with N^{3}LL ($m\alpha^6 \ln\alpha + m\alpha^7 \ln^2\alpha + \ldots$) precision[7].

We describe the energy levels of a nS ($l = 0$) state by dividing it up into a SI term called spin-average and a SD term called hyperfine splitting:

$$E_{\text{S-wave}}(J, n) = E_{\text{aver}}(n) + \mathbf{S}_1 \cdot \mathbf{S}_2 E_{\text{hfs}}(n)\,, \tag{1}$$

where J is the total spin value and $\mathbf{S}_1$, $\mathbf{S}_2$ are the spins of the fermion and the anti-fermion, respectively.

We will obtain partial results, whereas the missing contributions are expected to be small.

[7] C. Anzai, D. Moreno, and A. Pineda, Phys. Rev. D **98**, 114034 (2018).

pNRQCD Lagrangian

The most general pNRQCD Lagrangian compatible with the symmetries of QCD that can be constructed with a singlet and an octet quarkonium field, as well as an ultrasoft gluon field at NLO in the multipole expansion, has the form[8]

$$\begin{aligned}\mathcal{L}_{\rm pNRQCD} =& \int d^3\mathbf{r}\ \mathrm{Tr}\left\{ \mathrm{S}^\dagger\left(i\partial_0 - h_s(\mathbf{r},\mathbf{p},\mathbf{P_R},\mathbf{S}_1,\mathbf{S}_2)\right)\mathrm{S} + \mathrm{O}^\dagger\left(iD_0 - h_o(\mathbf{r},\mathbf{p},\mathbf{P_R},\mathbf{S}_1,\mathbf{S}_2)\right)\mathrm{O}\right\} \\ & + V_A(r)\mathrm{Tr}\left\{\mathrm{O}^\dagger\mathbf{r}\cdot g\mathbf{E}\,\mathrm{S} + \mathrm{S}^\dagger\mathbf{r}\cdot g\mathbf{E}\,\mathrm{O}\right\} + \frac{V_B(r)}{2}\mathrm{Tr}\left\{\mathrm{O}^\dagger\mathbf{r}\cdot g\mathbf{E}\,\mathrm{O} + \mathrm{O}^\dagger\mathrm{O}\mathbf{r}\cdot g\mathbf{E}\right\} \\ & - \frac{1}{4}G^a_{\mu\nu}G^{\mu\nu\,a} + \sum_{i=1}^{n_f}\bar{q}_i\, i\not{D}\, q_i\,, \end{aligned} \tag{2}$$

$$h_s(\mathbf{r},\mathbf{p},\mathbf{P_R},\mathbf{S}_1,\mathbf{S}_2) = \frac{\mathbf{p}^2}{2m_r} + \frac{\mathbf{P}_\mathbf{R}^2}{2M} + V_s(\mathbf{r},\mathbf{p},\mathbf{P_R},\mathbf{S}_1,\mathbf{S}_2), \tag{3}$$

$$h_o(\mathbf{r},\mathbf{p},\mathbf{P_R},\mathbf{S}_1,\mathbf{S}_2) = \frac{\mathbf{p}^2}{2m_r} + \frac{\mathbf{P}_\mathbf{R}^2}{2M} + V_o(\mathbf{r},\mathbf{p},\mathbf{P_R},\mathbf{S}_1,\mathbf{S}_2), \tag{4}$$

where h_s, V_s (h_o, V_o) are operators acting on the Hilbert space of a heavy quark-antiquark system in the singlet (octet) configuration.

[8] See A. Pineda, and J. Soto, Nucl. Phys. Proc. Suppl. **64**, 428 (1998) and N. Brambilla, A. Pineda, J. Soto, and A. Vairo, Nucl. Phys. **B566**, 275 (2000).

pNRQCD Lagrangian

The running of $\tilde{D}_d^{(2)}$ is sensitive to potential loops, which are more efficiently computed in momentum space. The singlet potential in momentum space can be expanded in powers of $1/m$ (up to logarithms):

$$\begin{aligned}
\tilde{V}_s \equiv \langle \mathbf{p}' | V_s | \mathbf{p} \rangle \quad = \quad & -4\pi C_F \frac{\alpha_{\tilde{V}}}{\mathbf{q}^2} - \mathbf{p}^4 \left(\frac{c_4^{(1)}}{8m_1^3} + \frac{c_4^{(2)}}{8m_2^3} \right) (2\pi)^d \delta^{(d)}(\mathbf{q}) \\
& - C_F C_A \tilde{D}^{(1)} \frac{\pi^2}{2m_r \, |\mathbf{q}|^{1-2\epsilon}} \\
& - \frac{2\pi C_F \tilde{D}_1^{(2)}}{m_1 m_2} \frac{\mathbf{p}^2 + \mathbf{p}'^2}{\mathbf{q}^2} + \frac{\pi C_F \tilde{D}_2^{(2)}}{m_1 m_2} \left(\left(\frac{\mathbf{p}^2 - \mathbf{p}'^2}{\mathbf{q}^2} \right)^2 - 1 \right) \\
& + \frac{\pi C_F \tilde{D}_d^{(2)}}{m_1 m_2} - \frac{4\pi C_F \tilde{D}_{S^2}^{(2)}}{d \, m_1 m_2} [\mathbf{S}_1^i, \mathbf{S}_1^j][\mathbf{S}_2^i, \mathbf{S}_2^j] \\
& + \frac{4\pi C_F \tilde{D}_{S_{12}}^{(2)}}{d \, m_1 m_2} [\mathbf{S}_1^i, \mathbf{S}_1^r][\mathbf{S}_2^i, \mathbf{S}_2^j] \left(\delta^{rj} - d \, \frac{\mathbf{q}^r \mathbf{q}^j}{\mathbf{q}^2} \right) \\
& - \frac{6\pi C_F}{m_1 m_2} \frac{\mathbf{p}^i \mathbf{q}^j}{\mathbf{q}^2} \left(\tilde{D}_{LS_1}^{(2)} [\mathbf{S}_1^i, \mathbf{S}_1^j] + \tilde{D}_{LS_2}^{(2)} [\mathbf{S}_2^i, \mathbf{S}_2^j] \right) ,
\end{aligned} \tag{5}$$

where m_1 (m_2) is the quark (antiquark) mass and $m_r = m_1 m_2/(m_1 + m_2)$ is the reduced mass of the system.

pNRQCD Lagrangian

where

- The Wilson coefficients $\tilde{D}$ stand for the Fourier transform of the Wilson coefficients in position space D.
- For them, and also for $\alpha_{\tilde{V}}$, we use the power counting LO/LL for the first nonvanishing correction, and so on.
- The computation of the NLL running of $\tilde{D}_d^{(2)}$ will require the use of the Wilson coefficients of the other potentials at LL. In the off-shell Coulomb[9] matching scheme they are given by

$$\alpha_V = \alpha_{\tilde{V}} = \alpha\,, \tag{6}$$

$$D_{\rm CG}^{(1)\,\rm LL} = \tilde{D}_{\rm CG}^{(1)\,\rm LL} = \alpha^2(\nu) + \frac{16}{3\beta_0}\left(\frac{C_A}{2} + C_F\right)\alpha^2(\nu)\ln\left(\frac{\alpha(\nu)}{\alpha(\nu^2/\nu_h)}\right)\,, \tag{7}$$

$$D_1^{(2)\,\rm LL} = \tilde{D}_1^{(2)\,\rm LL} = \alpha(\nu) + \frac{(m_1+m_2)^2}{m_1 m_2}\frac{2C_A}{3\beta_0}\alpha(\nu)\ln\left(\frac{\alpha(\nu)}{\alpha(\nu^2/\nu_h)}\right)\,, \tag{8}$$

$$D_{S_{12}}^{(2)\,\rm LL} = \tilde{D}_{S_{12}}^{(2)\,\rm LL} = \alpha(\nu)c_F^2(\nu)\,, \tag{9}$$

$$D_{S^2}^{(2)\,\rm LL} = \tilde{D}_{S^2}^{(2)\,\rm LL} = \alpha(\nu)c_F^2(\nu) - \frac{3}{2\pi C_F}(d_{sv}(\nu) + C_F d_{vv}(\nu))\,. \tag{10}$$

[9] which are equal to the Feynman at this order.

pNRQCD Lagrangian

The Wilson coefficient $\tilde{D}_d^{(2)}(\nu_h;\nu)$ can be written as the sum of the LL term and the NLL correction

$$\tilde{D}_d^{(2)}(\nu_h;\nu) = \tilde{D}_d^{(2)\,\mathrm{LL}}(\nu_h;\nu) + \delta\tilde{D}_d^{(2)\,\mathrm{NLL}}(\nu_h;\nu)\,, \tag{11}$$

and the NLL correction can be conveniently splitted into the following pieces

$$\begin{aligned} \delta\tilde{D}_d^{(2)\,\mathrm{NLL}}(\nu_h;\nu) \quad = \quad & \tilde{D}_d^{(2)\,\mathrm{NLO}}(\nu_h) \\ & +\delta\tilde{D}_{d,us}^{(2)\,\mathrm{NLL}}(\nu_h;\nu) + \delta\tilde{D}_{d,s}^{(2)\,\mathrm{NLL}}(\nu_h;\nu) + \delta\tilde{D}_{d,p}^{(2)\,\mathrm{NLL}}(\nu_h;\nu)\,, \end{aligned} \tag{12}$$

where $\tilde{D}_d^{(2)\,\mathrm{NLO}}(\nu_h)$ is the pure NLO matching condition and $\delta\tilde{D}_{d,us}^{(2)\,\mathrm{NLL}}(\nu_h;\nu)$, $\delta\tilde{D}_{d,s}^{(2)\,\mathrm{NLL}}(\nu_h;\nu)$ and $\delta\tilde{D}_{d,p}^{(2)\,\mathrm{NLL}}(\nu_h;\nu)$ stand for the NLL ultrasoft, soft and potential running of $\tilde{D}_d^{(2)}$. The second line is zero for $\nu=\nu_h$.

pNRQCD Lagrangian

The LL running is known[10]. In the off-shell Coulomb matching scheme:

$$\begin{aligned} D^{(2)\,\mathrm{LL}}_{d,\mathrm{CG}}(\nu) = \tilde{D}^{(2)\,\mathrm{LL}}_{d,\mathrm{CG}}(\nu) &= 2\alpha(\nu) + \frac{1}{\pi C_F}\left[d_{ss}(\nu) + C_F \bar{d}_{vs}(\nu)\right] \\ &+ \frac{(m_1+m_2)^2}{m_1 m_2}\frac{8}{3\beta_0}\left(\frac{C_A}{2} - C_F\right) \\ &\times \alpha(\nu)\ln\left(\frac{\alpha(\nu)}{\alpha(\nu^2/\nu_h)}\right), \end{aligned} \tag{13}$$

where

$$\bar{d}_{vs}(\nu) = \frac{1}{2}\pi\alpha(\nu) m_1 m_2 \left(\frac{c_D^{(1)}}{m_1^2} + \frac{c_D^{(2)}}{m_2^2}\right) + d_{vs}(\nu) \tag{14}$$

is a gauge invariant combination of NRQCD Wilson coefficients whose LL running is known[11].

[10] A. Pineda, Phys. Rev. D **65**, 074007 (2002)

[11] See A. Pineda, Phys. Rev. D **65**, 074007 (2002) and A. A. Penin, A. Pineda, V. A. Smirnov, and M. Steinhauser, Nucl. Phys. **B699**, 183 (2004); **B829**, 398(E) (2010).

pNRQCD Lagrangian

The initial matching condition at NLO, $\tilde{D}_d^{(2)\,\mathrm{NLO}}(\nu_h)$, is also known. In the Coulomb gauge matching scheme is given by

$$\begin{aligned}\tilde{D}_{d,\mathrm{CG}}^{(2)\,\mathrm{NLO}}(\nu_h) \quad = \quad & \frac{\alpha^2(\nu_h)}{4\pi}\left(\frac{62}{9}C_A + \frac{4}{3}C_F - \frac{32}{3}C_A\ln 2 - \frac{28}{9}T_F n_f\right. \\ & + \left(\frac{m_1}{m_2} + \frac{m_2}{m_1}\right)\left[-\frac{10}{9}T_F n_f + \left(\frac{61}{18} - \frac{16}{3}\ln 2\right)C_A\right]\Bigg) \\ & + \frac{1}{\pi C_F}\left(d_{ss}(\nu_h) + C_F\bar{d}_{vs}(\nu_h)\right) \,. \qquad (15)\end{aligned}$$

The NRQCD Wilson coefficients c_D, d_{ss} and d_{vs} are known at one-loop order[12].

[12] A. V. Manohar, Phys. Rev. D **56**, 230 (1997); A. Pineda, and J. Soto, Phys. Rev. D **58**, 114011 (1998).

pNRQCD Lagrangian

At present, the NLL running of $\tilde{D}_d^{(2)}$ is known for the ultrasoft term[13]

$$\begin{aligned}
\delta\tilde{D}_{d,us}^{(2)\,\mathrm{NLL}}(\nu_h;\nu) &= \frac{(m_1+m_2)^2}{m_1 m_2}\frac{4\pi}{\beta_0}\left(\frac{C_A}{2}-C_F\right)\alpha(\nu) \\
&\times\left\{\frac{2}{3\pi}\ln\left(\frac{\alpha(\nu)}{\alpha(\nu^2/\nu_h)}\right)a_1\frac{\alpha(\nu)}{4\pi}+(\alpha(\nu^2/\nu_h)-\alpha(\nu))\right. \\
&\times\left.\left(\frac{8}{3}\frac{\beta_1}{\beta_0}\frac{1}{(4\pi)^2}-\frac{1}{27\pi^2}\left(C_A\left(47+6\pi^2\right)-10T_F n_f\right)\right)\right\},
\end{aligned} \tag{16}$$

where $a_1 = 31C_A/9 - 20T_F n_f/9$. Whereas

- The soft running $\delta\tilde{D}_{d,s}^{(2)\,\mathrm{NLL}}(\nu_h;\nu)$
- The potential running $\delta\tilde{D}_{d,p}^{(2)\,\mathrm{NLL}}(\nu_h;\nu)$

are the missing terms to obtain the complete NLL running of $\tilde{D}_d^{(2)}$.

[13] A. Pineda, Phys. Rev. D **84**, 014012 (2011).

Matching NRQCD with pNRQCD: The SI potential

We need to compute the unknown SI potentials whose expectation values produce corrections to the $\mathcal{O}(m\alpha^6)$ spectrum, only paying attention to those that produce logarithmically enhanced $\mathcal{O}(m\alpha^6 \ln\alpha + \ldots)$ corrections to the S-wave spin-average spectrum.

- **The $\mathcal{O}(\alpha/m^4)$, $\mathcal{O}(\alpha^2/m^3)$ potentials:** finite, produce logarithmically enhanced corrections through potential loops, whose divergences get aborbed in $\tilde{D}_d^{(2)}$ (potential running).
- **The $\mathcal{O}(\alpha^3/m^2)$ potential:** divergent, logarithmic enhanced corrections not generated by potential loops but by the divergent structure of the potential itself. Divergences are also absorbed by $\tilde{D}_d^{(2)}$ (soft running).
- **The p^6/m^5 correction to the kinetic term:** It does not produce ultraviolet divergences, so it does not has to be considered.

$\mathcal{O}(\alpha/m^4)$ potential

From a NRQCD tree level computation (see topology (a)) we obtain the complete SI $\mathcal{O}(\alpha/m^4)$ potential in momentum space and in the Coulomb gauge.

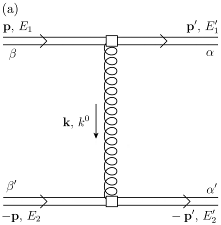

Figure: Topology that contributes to the tree level potential. Properly changing the vertex and/or Taylor expanding the denominator of the propagators all potentials are generated.

$\mathcal{O}(\alpha/m^4)$ potential

It reads

$$\begin{aligned}
\tilde{V}_{\rm tree} \quad = \quad & -c_D^{(1)}c_D^{(2)}C_F\frac{g^2}{64m_1^2m_2^2}\mathbf{k}^2 \\
& -C_F g^2\left(\frac{c_{X1}^{(1)}}{m_1^4}+\frac{c_{X1}^{(2)}}{m_2^4}\right)\frac{(\mathbf{p}^2-\mathbf{p}'^{\,2})^2}{\mathbf{k}^2} \\
& -C_F g^2\left(\frac{c_{X2}^{(1)}}{m_1^4}+\frac{c_{X2}^{(2)}}{m_2^4}\right)(\mathbf{p}^2+\mathbf{p}'^2) \\
& -C_F g^2\left(\frac{c_{X3}^{(1)}}{m_1^4}+\frac{c_{X3}^{(2)}}{m_2^4}\right)\mathbf{k}^2 \\
& +C_F\frac{g^2c_k^{(1)2}c_k^{(2)2}}{16m_1^2m_2^2}\frac{1}{\mathbf{k}^4}(\mathbf{p}^2-\mathbf{p}'^2)^2\left(2(\mathbf{p}^2+\mathbf{p}'^2)-\mathbf{k}^2-\frac{(\mathbf{p}^2-\mathbf{p}'^2)^2}{\mathbf{k}^2}\right) \\
& +C_F\frac{g^2}{16m_1m_2}\left(\frac{c_4^{(1)}c_k^{(2)}}{m_1^2}+\frac{c_4^{(2)}c_k^{(1)}}{m_2^2}\right)\frac{\mathbf{p}^2+\mathbf{p}'^2}{\mathbf{k}^2}\left(2(\mathbf{p}^2+\mathbf{p}'^2)-\mathbf{k}^2-\frac{(\mathbf{p}^2-\mathbf{p}'^2)^2}{\mathbf{k}^2}\right) \\
& -C_F\frac{g^2}{16m_1m_2}\left(\frac{c_M^{(1)}c_k^{(2)}}{m_1^2}+\frac{c_M^{(2)}c_k^{(1)}}{m_2^2}\right)\left(\frac{(\mathbf{p}^2-\mathbf{p}'^2)^2}{\mathbf{k}^2}-(\mathbf{p}+\mathbf{p}')^2\right).
\end{aligned} \tag{17}$$

$\mathcal{O}(\alpha/m^4)$ potential

- The $1/m^4$ potentials generated by the dimension eight four-heavy fermion NRQCD Lagrangian operators can be neglected (do not produce potential loops).
- Incorporating the LL running of the HQET Wilson coefficients, these potentials are RG improved.
- Note that these potentials are also valid for QED.

$\mathcal{O}(\alpha^2/m^3)$ potential

We now compute the $\mathcal{O}(\alpha^2/m^3)$ SI potential in the Coulomb gauge. The NRQCD topologies that contribute are the following.

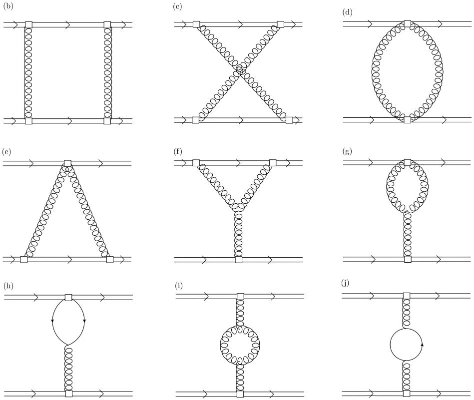

Figure: Topologies that contribute to the $\mathcal{O}(\alpha^2/m^3)$ potential. Properly changing the vertices and/or Taylor expanding the propagators, all potentials are generated.

$\mathcal{O}(\alpha^2/m^3)$ potential

The (c)-type diagrams generate the following $\mathcal{O}(\alpha^2/m^3)$ potentials:

$$\begin{aligned} \tilde{V}^{(c,1)}_{\rm 1loop} &= -C_F\left(C_F-\frac{C_A}{2}\right)c_k^{(1)}c_k^{(2)}\frac{g^4}{512m_1m_2}\frac{E_1+E_2}{|\mathbf{k}|^{3-2\epsilon}} \\ &\times\left(2(\mathbf{p}^2+\mathbf{p}'^2)-\mathbf{k}^2-\frac{(\mathbf{p}^2-\mathbf{p}'^2)^2}{\mathbf{k}^2}-\frac{8(\mathbf{p}\cdot\mathbf{k})(\mathbf{p}'\cdot\mathbf{k})}{\mathbf{k}^2}\right)\,, \end{aligned} \tag{18}$$

$$\begin{aligned} \tilde{V}^{(c,2)}_{\rm 1loop} &= -C_F\left(C_F-\frac{C_A}{2}\right)\frac{g^4}{256m_1m_2}\left(\frac{c_k^{(1)\,2}c_k^{(2)}}{m_1}+\frac{c_k^{(1)}c_k^{(2)\,2}}{m_2}\right)|\mathbf{k}|^{1+2\epsilon} \\ &\times\left(3(\mathbf{p}^2+\mathbf{p}'^2)\frac{(\mathbf{p}\cdot\mathbf{k})(\mathbf{p}'\cdot\mathbf{k})}{\mathbf{k}^6}-\frac{2(\mathbf{p}^2+\mathbf{p}'^2)}{\mathbf{k}^2}+\frac{11}{4}\right. \\ &\left.-\frac{1}{4}\frac{(\mathbf{p}^2-\mathbf{p}'^2)^2}{\mathbf{k}^4}-\frac{1}{2}\frac{(\mathbf{p}^2+\mathbf{p}'^2)^2}{\mathbf{k}^4}\right)\,. \end{aligned} \tag{19}$$

$\mathcal{O}(\alpha^2/m^3)$ potential

The (e)-type diagrams generate the following $\mathcal{O}(\alpha^2/m^3)$ potentials:

$$\begin{aligned}\tilde{V}^{(e,1)}_{1\mathrm{loop}} &= C_F\left(2C_F-\frac{C_A}{2}\right)\frac{g^4}{512m_1m_2}\left(\frac{c_k^{(1)\,2}c_k^{(2)}}{m_1}+\frac{c_k^{(1)}c_k^{(2)\,2}}{m_2}\right)|\mathbf{k}|^{1+2\epsilon}\\ &\times\left(\frac{5(\mathbf{p}^2+\mathbf{p}'^2)}{\mathbf{k}^2}-\frac{7}{2}-\frac{3}{2}\frac{(\mathbf{p}^2-\mathbf{p}'^2)^2}{\mathbf{k}^4}\right),\end{aligned} \tag{20}$$

$$\begin{aligned}\tilde{V}^{(e,2)}_{1\mathrm{loop}} &= \Bigg[-C_F\left(2C_F-\frac{C_A}{2}\right)\frac{g^4}{256}\left(\frac{c_{A_1}^{(1)}}{m_1^3}+\frac{c_{A_1}^{(2)}}{m_2^3}\right)\\ &-C_F\left(2C_F-\frac{C_A}{2}\right)\frac{g^4}{512}\left(\frac{c_{A_2}^{(1)}}{m_1^3}+\frac{c_{A_2}^{(2)}}{m_2^3}\right)\\ &-C_F\left(2C_F-\frac{C_A}{2}\right)\frac{g^4}{128m_1m_2}\left(\frac{c_F^{(1)\,2}c_k^{(2)}}{m_1}+\frac{c_F^{(2)\,2}c_k^{(1)}}{m_2}\right)\\ &-C_FC_A\frac{g^4}{256m_1m_2}\left(\frac{c_D^{(1)}c_k^{(2)}}{m_1}+\frac{c_D^{(2)}c_k^{(1)}}{m_2}\right)\\ &-\frac{T_F}{N_c}C_F\frac{g^4}{128}\left(\frac{c_{A_3}^{(1)}}{m_1^3}+\frac{c_{A_3}^{(2)}}{m_2^3}\right)-\frac{T_F}{N_c}C_F\frac{g^4}{256}\left(\frac{c_{A_4}^{(1)}}{m_1^3}+\frac{c_{A_4}^{(2)}}{m_2^3}\right)\Bigg]|\mathbf{k}|^{1+2\epsilon}.\end{aligned} \tag{21}$$

$\mathcal{O}(\alpha^2/m^3)$ potential

The (f)-type diagrams generate the following $\mathcal{O}(\alpha^2/m^3)$ potentials:

$$\tilde{V}^{(f,1)}_{\rm 1loop} = -C_F C_A \frac{g^4}{128}\left(\frac{c_F^{(1)\,2} c_k^{(1)}}{m_1^3} + \frac{c_F^{(2)\,2} c_k^{(2)}}{m_2^3}\right)|\mathbf{k}|^{1+2\epsilon}\frac{\mathbf{p}\cdot\mathbf{p}'}{\mathbf{k}^2}\,, \tag{22}$$

$$\begin{aligned}
\tilde{V}^{(f,2)}_{\rm 1loop} \quad = \quad & -C_F C_A \frac{g^4}{512 m_1 m_2}\left(\frac{c_k^{(2)} c_k^{(1)\,2}}{m_1} + \frac{c_k^{(1)} c_k^{(2)\,2}}{m_2}\right)|\mathbf{k}|^{1+2\epsilon}\left(1 - \frac{3}{2}\frac{\mathbf{p}^2+\mathbf{p}'^2}{\mathbf{k}^2}\right) \\
& \times\left(\frac{2(\mathbf{p}^2+\mathbf{p}'^2)}{\mathbf{k}^2} - 1 - \frac{(\mathbf{p}^2-\mathbf{p}'^2)^2}{\mathbf{k}^4}\right) \\
& -C_F C_A \frac{g^4}{512}\left(\frac{c_k^{(1)\,3}}{m_1^3} + \frac{c_k^{(2)\,3}}{m_2^3}\right)|\mathbf{k}|^{1+2\epsilon}\left(\frac{\mathbf{p}\cdot\mathbf{p}'}{\mathbf{k}^2} + \frac{5(\mathbf{p}\cdot\mathbf{k})(\mathbf{p}'\cdot\mathbf{k})}{\mathbf{k}^4} - \frac{12(\mathbf{p}\cdot\mathbf{p}')^2}{\mathbf{k}^4}\right. \\
& \left. + \frac{2\mathbf{p}^2\mathbf{p}'^2}{\mathbf{k}^4} + \frac{6(\mathbf{p}\cdot\mathbf{p}')(\mathbf{p}\cdot\mathbf{k})(\mathbf{p}'\cdot\mathbf{k})}{\mathbf{k}^6}\right),
\end{aligned} \tag{23}$$

$\mathcal{O}(\alpha^2/m^3)$ potential

$$\begin{aligned}
\tilde{V}^{(f,3)}_{1\mathrm{loop}} &= -c_k^{(1)} c_k^{(2)} C_F C_A \frac{3g^4}{128 m_1 m_2} |\mathbf{k}|^{-1+2\epsilon} \left(\mathbf{p}\cdot\mathbf{p}' - \frac{(\mathbf{p}\cdot\mathbf{k})(\mathbf{p}'\cdot\mathbf{k})}{\mathbf{k}^2} \right) \\
&\times \frac{(E_1+E_1')+(E_2+E_2')}{\mathbf{k}^2} \\
&- C_F C_A \frac{g^4}{256} \left(\frac{c_k^{(1)\,2}}{m_1^2}(E_1+E_1') + \frac{c_k^{(2)\,2}}{m_2^2}(E_2+E_2') \right) |\mathbf{k}|^{-1+2\epsilon} \\
&\times \left(\frac{5\mathbf{p}\cdot\mathbf{p}'}{\mathbf{k}^2} - \frac{3(\mathbf{p}\cdot\mathbf{k})(\mathbf{p}'\cdot\mathbf{k})}{\mathbf{k}^4} \right), \qquad (24)
\end{aligned}$$

$$\begin{aligned}
\tilde{V}^{(f,4)}_{1\mathrm{loop}} &= -C_F C_A \frac{g^4}{256} \left(\frac{c_k^{(1)\,3}}{m_1^3} + \frac{c_k^{(2)\,3}}{m_2^3} \right) |\mathbf{k}|^{1+2\epsilon} \Bigg(-1 + \frac{\mathbf{p}^2+\mathbf{p}'^2}{\mathbf{k}^2} \\
&+ \frac{3(\mathbf{p}^4+\mathbf{p}'^4)+(\mathbf{p}^2+\mathbf{p}'^2)(\mathbf{p}\cdot\mathbf{p}')-6(\mathbf{p}\cdot\mathbf{p}')^2}{\mathbf{k}^4} \\
&+ \frac{-3(\mathbf{p}^6+\mathbf{p}'^6)+4(\mathbf{p}^4+\mathbf{p}'^4)(\mathbf{p}\cdot\mathbf{p}')-2(\mathbf{p}\cdot\mathbf{p}')^3}{\mathbf{k}^6} \Bigg), \qquad (25)
\end{aligned}$$

$\mathcal{O}(\alpha^2/m^3)$ potential

$$
\begin{aligned}
\tilde{V}^{(f,5)}_{1\mathrm{loop}} &= -C_F C_A \frac{g^4}{128}|\mathbf{k}|^{1+2\epsilon}\left[\frac{c_k^{(2)\,2}}{m_2^2}\left(\frac{3(E_1+E_1')(\mathbf{p}\cdot\mathbf{k})(\mathbf{p}'\cdot\mathbf{k})}{\mathbf{k}^6}+\frac{(E_1+E_1')(\mathbf{p}\cdot\mathbf{p}')}{\mathbf{k}^4}\right.\right.\\
&\quad\left.+\frac{2(E_1\mathbf{p}^4+E_1'\mathbf{p}'^4)}{\mathbf{k}^6}-\frac{2(E_1\mathbf{p}^2+E_1'\mathbf{p}'^2)(\mathbf{p}\cdot\mathbf{p}'+\mathbf{k}^2)}{\mathbf{k}^6}\right)\\
&\quad+\frac{c_k^{(1)\,2}}{m_1^2}\left(\frac{3(E_2+E_2')(\mathbf{p}\cdot\mathbf{k})(\mathbf{p}'\cdot\mathbf{k})}{\mathbf{k}^6}+\frac{(E_2+E_2')(\mathbf{p}\cdot\mathbf{p}')}{\mathbf{k}^4}+\frac{2(E_2\mathbf{p}^4+E_2'\mathbf{p}'^4)}{\mathbf{k}^6}\right.\\
&\quad\left.\left.-\frac{2(E_2\mathbf{p}^2+E_2'\mathbf{p}'^2)(\mathbf{p}\cdot\mathbf{p}'+\mathbf{k}^2)}{\mathbf{k}^6}\right)\right], \qquad (26)
\end{aligned}
$$

$$
\begin{aligned}
\tilde{V}^{(f,6)}_{1\mathrm{loop}} &= -C_F C_A \frac{7g^4}{256 m_1 m_2}\left(\frac{c_k^{(1)\,2}c_k^{(2)}}{m_1}+\frac{c_k^{(1)}c_k^{(2)\,2}}{m_2}\right)|\mathbf{k}|^{1+2\epsilon}\\
&\quad\times\left(\frac{2(\mathbf{p}^2+\mathbf{p}'^2)}{\mathbf{k}^2}-1-\frac{(\mathbf{p}^2-\mathbf{p}'^2)^2}{\mathbf{k}^4}\right), \qquad (27)
\end{aligned}
$$

$\mathcal{O}(\alpha^2/m^3)$ potential

$$
\begin{aligned}
\tilde{V}^{(f,7)}_{1\rm loop} \quad = \quad & C_F C_A \frac{g^4}{256 m_1 m_2}\left(\frac{c_D^{(1)} c_k^{(2)}}{m_1} + \frac{c_D^{(2)} c_k^{(1)}}{m_2}\right)|\mathbf{k}|^{1+2\epsilon} \\
& + C_F C_A \frac{g^4}{1024}\left(\frac{c_4^{(1)}}{m_1^3} + \frac{c_4^{(2)}}{m_2^3}\right)|\mathbf{k}|^{1+2\epsilon}\left(\frac{10(\mathbf{p}^2 + \mathbf{p}'^2)}{\mathbf{k}^2} - 7 + \frac{5(\mathbf{p}^2 - \mathbf{p}'^2)^2}{\mathbf{k}^4}\right) \\
& - C_F C_A \frac{g^4}{256}\left(\frac{c_M^{(1)}}{m_1^3} + \frac{c_M^{(2)}}{m_2^3}\right)|\mathbf{k}|^{1+2\epsilon} \\
& - C_F C_A \frac{g^4}{512}\left(\frac{c_F^{(1)} c_S^{(1)}}{m_1^3} + \frac{c_F^{(2)} c_S^{(2)}}{m_2^3}\right)|\mathbf{k}|^{1+2\epsilon} \,, \qquad (28)
\end{aligned}
$$

$$
\tilde{V}^{(f,8)}_{1\rm loop} = C_F C_A \frac{g^4}{64}|\mathbf{k}|^{-5+2\epsilon}\left[\left(c_k^{(1)}\frac{E_1^2}{m_1} + c_k^{(2)}\frac{E_2^2}{m_2}\right)(\mathbf{p}\cdot\mathbf{k}) - \left(c_k^{(1)}\frac{E_1'^2}{m_1} + c_k^{(2)}\frac{E_2'^2}{m_2}\right)(\mathbf{p}'\cdot\mathbf{k})\right], \qquad (29)
$$

$$
\tilde{V}^{(f,9)}_{1\rm loop} = C_F C_A \frac{g^4}{128}\left(\frac{c_F^{(1)\,2}}{m_1^2}(E_1 + E_1') + \frac{c_F^{(2)\,2}}{m_2^2}(E_2 + E_2')\right)|\mathbf{k}|^{-1+2\epsilon} \,. \qquad (30)
$$

$\mathcal{O}(\alpha^2/m^3)$ potential

- The rest of the topologies: (b), (d), (g), (h), (i) and (j), do not contribute.
- As we have incorporated the LL running of the HQET Wilson coefficients[14], these potentials are already RG improved.
- These potentials are also valid for QED.
- Note that some potentials are energy dependent. Such energy dependence can be eliminated by using field redefinitions/full EOMs (free + Coulomb potential).

[14] D. Moreno, and A. Pineda, Phys. Rev. D **97** 016012 (2018); **98** 059902(E) (2018).

Equations of motion

Let us consider the energy dependent potentials proportional to c_F^2 (c_k^2 only included partially because the α^3/m^2 potential proportional to c_k^2 will be missing anyway[15]).

By using the free on-shell EOMs we find a new $\mathcal{O}(\alpha^2/m^3)$ potential

$$\tilde{V}^{(f,9)}_{1\text{loop}} = C_F C_A \frac{g^4}{256}\left(\frac{c_F^{(1)\,2} c_k^{(1)}}{m_1^3} + \frac{c_F^{(2)\,2} c_k^{(2)}}{m_2^3}\right) |\mathbf{k}|^{1+2\epsilon} \frac{\mathbf{p}^2 + \mathbf{p}'^2}{\mathbf{k}^2} \,. \tag{31}$$

From the Coulomb term in the EOMs a new $\mathcal{O}(\alpha^3/m^2)$ potential is generated. We only care about the divergent part because we are only interested in logarithmically enhanced contributions to the spectrum:

$$\delta\tilde{V}^{(f,9)}_{1\text{loop}} = \frac{1}{32} C_F^2 C_A \frac{g^6 k^{4\epsilon}}{(4\pi)^2}\left(\frac{c_F^{(1)2}}{m_1^2} + \frac{c_F^{(2)2}}{m_2^2}\right) \frac{1}{\epsilon} \,. \tag{32}$$

We checked that this result does not depend on the gauge.

[15] And it could depend on the matching scheme, which is different for the potential and soft RGEs. So, we postpone its incorporation to have the full result.

$\mathcal{O}(\alpha^3/m^2)$ delta-like potential

- Finally, we perform a partial computation (terms proportional to $\bar{c}_1^{hl}$ and c_F) of the $\mathcal{O}(\alpha^3/m^2)$ soft contribution to the SI delta-like potential.

- To that purpose, we need to compute the divergent part of the matching between NRQCD and pNRQCD at two loops and at $\mathcal{O}(1/m^2)$.

- The computation is done with a general gauge parameter ξ in the kinematic configuration $\mathbf{p} = \mathbf{k}$ and $\mathbf{p}' = 0$.

- We also set the external energy to zero, because it produces subleading corrections.

- The result vanishes in QED.

$\mathcal{O}(\alpha^3/m^2)$ delta-like potential

- We performed the non-trivial checks:
  - That c_D and c_1^{hl} appear in the gauge invariant combination $\bar{c}_1^{hl} = c_D + c_1^{hl}$.
  - That the counterterm is independent of k and that the $1/\epsilon^2$ terms comply with the constraints from the RG.
  - That the result is independent of the gauge fixing parameter ξ.
- The terms proportional to c_k^2, d_{ss} and d_{vs} have not been computed.
- The missing terms must be computed in a way consistent with the scheme used for the α^2/m^3 potential, as a strong mixing of the terms proportional to c_k^2 is expected after using the EOMs.

NLL running of $\tilde{D}_d^{(2)}$

Now we compute the NLL soft and potential running of $\tilde{D}_d^{(2)}$:

- $\delta\tilde{D}_{d,s}^{(2)\,\mathrm{NLL}}$
- $\delta\tilde{D}_{d,p}^{(2)\,\mathrm{NLL}}$

Soft running

From the divergent part of the $\mathcal{O}(\alpha^3/m^2)$ potential we can obtain the $\mathcal{O}(\alpha^3)$ soft RGE of $\tilde{D}_d^{(2)}$ proportional to c_F^2 and $\bar{c}_1^{hl}$. It reads

$$
\begin{aligned}
&\nu \frac{d}{d\nu}\tilde{D}_d^{(2)}\Big|_{\text{soft}} = \frac{\alpha^2}{\pi}\left(2C_F - \frac{C_A}{2}\right)c_k^{(1)}c_k^{(2)} \\
&+\frac{\alpha^2}{\pi}\left[\frac{m_1}{m_2}\left(\frac{1}{3}T_f n_f \bar{c}_1^{hl(2)} - \frac{4}{3}(C_A+C_F)[c_k^{(2)}]^2 - \frac{5}{12}C_A[c_F^{(2)}]^2\right)\right. \\
&\qquad\left.+\frac{m_2}{m_1}\left(\frac{1}{3}T_f n_f \bar{c}_1^{hl(1)} - \frac{4}{3}(C_A+C_F)[c_k^{(1)}]^2 - \frac{5}{12}C_A[c_F^{(1)}]^2\right)\right] \\
&+\frac{\alpha^3}{4\pi^2}\left[\frac{m_1}{m_2}\left(-\frac{T_F n_f}{54}(65C_A - 54C_F)\bar{c}_1^{hl(2)} - \frac{C_A}{18}(25C_A - \frac{125}{3}T_F n_f)[c_F^{(2)}]^2\right)\right. \\
&\qquad\left.+\frac{m_2}{m_1}\left(-\frac{T_F n_f}{54}(65C_A - 54C_F)\bar{c}_1^{hl(1)} - \frac{C_A}{18}(25C_A - \frac{125}{3}T_F n_f)[c_F^{(1)}]^2\right)\right] \\
&+\mathcal{O}(\alpha^3)\,.
\end{aligned}
\tag{33}
$$

- The $\mathcal{O}(\alpha^3)$ stands for missing terms proportional to NRQCD Wilson coefficients different from c_F^2 and $\bar{c}_1^{hl}$ i.e c_k, d_{ss} and d_{vs}.
- We compute the strict NLL contribution $\delta\tilde{D}_{d,s}^{(2)\,\mathrm{NLL}}$ to the solution of this equation (the LL is already included in Eq. (13)).

Soft running

One should also add the contributions generated by the new α^3/m^2 potentials (Eq. (32)) appearing after using the EOMs[16] in energy dependent potentials:

$$\nu \frac{d}{d\nu} \tilde{D}_d^{(2)} \Big|_{\rm soft} = \cdots + \frac{1}{4} C_F C_A \alpha^3 \left(\frac{m_2}{m_1} c_F^{(1)\,2} + \frac{m_1}{m_2} c_F^{(2)\,2} \right) , \tag{34}$$

where the dots stand for the already computed soft RGE. Its solution reads

$$\delta \tilde{D}_{d,new}^{(2)\,\rm NLL} = -\frac{\pi C_A C_F (m_1^2 + m_2^2)(1 - z^{-2(C_A - \beta_0)}) \alpha^2(\nu_h)}{4 m_1 m_2 (C_A - \beta_0)} . \tag{35}$$

where $z \equiv (\alpha(\nu)/\alpha(\nu_h))^{1/\beta_0}$.

The soft running will change to $\delta \tilde{D}_{d,s}^{(2)\,\rm NLL} \to \delta \tilde{D}_{d,s}^{(2)\,\rm NLL} + \delta \tilde{D}_{d,new}^{(2)\,\rm NLL}$.

[16] Remember that we only computed the potentials proportional to c_F^2 and $\bar{c}_1^{hl}$ (the latter is zero). The c_k^2 terms can also mix with the α^2/m^3 potentials through field redefinitions. This contribution could depend on the matching scheme, though.

Potential running

To determine the potential RGE, we need to compute all potential loops that produce UV divergences that get absorbed in $\tilde{D}_d^{(2)}$ and that are at most of $\mathcal{O}(\alpha^3)$.

- Since the delta-like potential is of $\mathcal{O}(1/m^2)$, we must construct potential loop diagrams of $\mathcal{O}(\alpha^n/m^2)$ with $n \leq 3$,

considering the power of α and m of each potential and that every propagator adds an extra power of the mass in the numerator.

Potential running

The diagrams that contribute to the NLL potential running of $\tilde{D}_d^{(2)}$ are the following

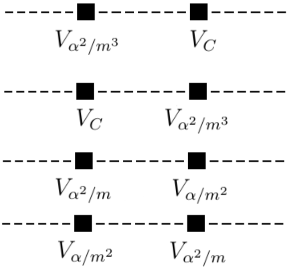

Figure: Divergent diagrams with one potential loop that contribute to the running of $\tilde{D}_d^{(2)}$ at $\mathcal{O}(\alpha^3)$.

Potential running

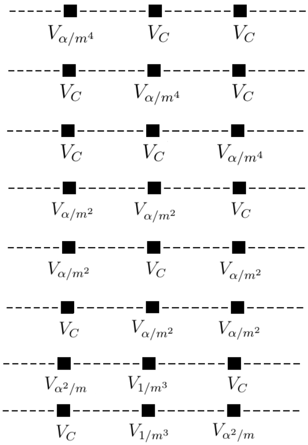

Figure: Divergent diagrams with two potential loops that contribute to the running of $\tilde{D}_d^{(2)}$ at $\mathcal{O}(\alpha^3)$.

Potential running

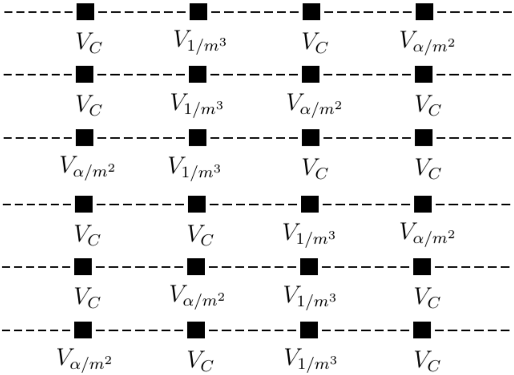

Figure: Divergent diagrams with three potential loops that contribute to the running of $\tilde{D}_d^{(2)}$ at $\mathcal{O}(\alpha^3)$.

Potential running

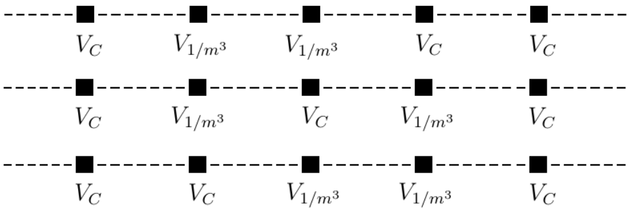

Figure: Divergent diagrams with four potential loops that contribute to the running of $\tilde{D}_d^{(2)}$ at $\mathcal{O}(\alpha^3)$.

where V_C is the tree level $\mathcal{O}(\alpha)$ Coulomb potential, V_{α^r/m^s} is the $\mathcal{O}(\alpha^r/m^s)$ potential and V_{1/m^3} corresponds to the first relativistic correction to the kinetic energy, which is proportional to c_4.

Potential running

We find that:

- The first contribution to the potential running is of $\mathcal{O}(\alpha^3)$.

- The UV divergences of such diagrams must be absorbed by all the $1/m^2$ potentials but, after the computation, we observe that all of them are absorbed only by the delta-like potential.

Potential running

- The potential RGE reads[17]

$$
\begin{aligned}
\nu \frac{d}{d\nu}\delta\tilde{D}_{d,p}^{(2)\,\mathrm{NLL}} &= -2c_4 C_F^2\alpha_V^2 m_r^3\left(\frac{1}{m_1^3}+\frac{1}{m_2^3}\right)\tilde{D}_d^{(2)} \\
&+C_F^2\alpha_{V_s}\frac{m_r^2}{m_1 m_2}\left(\tilde{D}_d^{(2)\,2} - 8\tilde{D}_d^{(2)}\tilde{D}_1^{(2)} + 12\tilde{D}_1^{(2)\,2} - \frac{5}{6}\tilde{D}_{S_{12}}^{(2)\,2} + \frac{4}{3}\tilde{D}_{S^2}^{(2)\,2}\right) \\
&+2c_4 C_F^2\alpha_V^2 m_r^3\left(\frac{1}{m_1^3}+\frac{1}{m_2^3}\right)\left(4\tilde{D}_1^{(2)}\right) \\
&+C_F C_A\left[2\tilde{D}_1^{(2)}\tilde{D}^{(1)} - \tilde{D}_d^{(2)}\tilde{D}^{(1)} + c_4\tilde{D}^{(1)}\alpha_V m_r m_1 m_2\left(\frac{1}{m_1^3}+\frac{1}{m_2^3}\right)\right] \\
&+c_4^2 C_F^2\alpha_V^3 m_r^4 m_1 m_2\left(\frac{1}{m_1^3}+\frac{1}{m_2^3}\right)^2 \\
&+\left(\frac{m_1}{m_2}+\frac{m_2}{m_1}\right)\frac{C_A^2(C_A-2C_F)\alpha^3}{2}D_{\mathbf{S}^2,1/r^3}^{(2)} \\
&-2C_F^2\alpha^3 m_r^2\left[\frac{5}{8}m_1 m_2\left(\frac{1}{m_1^4}+\frac{1}{m_2^4}\right) + 2\left(\frac{c_4^{(1)}}{m_1^2}+\frac{c_4^{(2)}}{m_2^2}\right) + \frac{1}{m_1 m_2}\right]
\end{aligned}
$$

[17] For simplicity, we use $c_k^{(i)} = 1$. See M. E. Luke, and A. V. Manohar, Phys. Lett. B **286**, 348 (1992).

Potential running

$$
\begin{aligned}
&+C_F\left(2C_F-\frac{C_A}{2}\right)\alpha^3 m_r m_1 m_2\left[\frac{1}{2}\left(\frac{c_{A_1}^{(1)}}{m_1^3}+\frac{c_{A_1}^{(2)}}{m_2^3}\right)+\frac{1}{4}\left(\frac{\bar{c}_{A_2}^{(1)}}{m_1^3}+\frac{\bar{c}_{A_2}^{(2)}}{m_2^3}\right)\right.\\
&\left.+\frac{1}{m_1 m_2}\left(\frac{c_F^{(1)\,2}}{m_1}+\frac{c_F^{(2)\,2}}{m_2}\right)\right]-\frac{1}{2}C_F C_A\alpha^3 m_r m_1 m_2\left[2\left(\frac{c_4^{(1)}}{m_1^3}+\frac{c_4^{(2)}}{m_2^3}\right)+\left(\frac{1}{m_1^3}+\frac{1}{m_2^3}\right)\right.\\
&\left.+\left(\frac{c_F^{(1)\,2}}{m_1^3}+\frac{c_F^{(2)\,2}}{m_2^3}\right)-\left(\frac{c_F^{(1)}c_S^{(1)}}{m_1^3}+\frac{c_F^{(2)}c_S^{(2)}}{m_2^3}\right)\right]\\
&-\left(C_F-\frac{C_A}{2}\right)C_F\alpha^3 m_r m_1 m_2\left[\left(\frac{c_{A_3}^{(1)}}{m_1^3}+\frac{c_{A_3}^{(2)}}{m_2^3}\right)+\frac{1}{2}\left(\frac{c_{A_4}^{(1)}}{m_1^3}+\frac{c_{A_4}^{(2)}}{m_2^3}\right)\right],
\end{aligned}
\tag{36}
$$

- Part of this equation was already computed in A. V. Manohar, and I. W. Stewart, Phys. Rev. Lett. **85**, 2248 (2000) with which we find agreement.

- The QED limit of several of these terms can also be checked with the computations done in I. B. Khriplovich, A. I. Milstein, and A. S. Yelkhovsky, Phys. Scr. **T46**, 252, (1993) with which we find agreement.

Potential running

Comments:

- The sixth line is a term generated by a divergent potential originated by the following ultrasoft diagram[18]

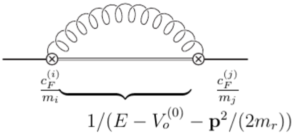

where

$$D_{\mathbf{S}^2,1/r^3} = \frac{1}{2C_A}\left[\left(\frac{\alpha(\nu_h)}{\alpha(\nu^2/\nu_h)}\right)^{2C_A/\beta_0} - \left(\frac{\alpha(\nu_h)}{\alpha(\nu)}\right)^{2C_A/\beta_0}\right]. \tag{37}$$

[18] A. A. Penin, A. Pineda, V. A. Smirnov, and M. Steinhauser, Nucl. Phys. **B699**, 183 (2004); **B829**, 398(E) (2010).

Potential running

- Note that the gauge-dependent Wilson coefficients c_{A_2}, c_D, c_M and c_{X1} appear[19].

- However, using reparametrization invariance[20] relations, everything can be written in terms of $\bar{c}_{A_2} = c_{A_2} - 4c_M$, which is gauge independent[21]. This is a strong check of the computation.

- In order to solve the potential RGE, we need to introduce the Wilson coefficients of the potentials with LL accuracy.

[19] D. Moreno, and A. Pineda, Phys. Rev. D **97** 016012 (2018); **98** 059902(E) (2018); R. J. Hill, G. Lee, G. Paz, and M. P. Solon, Phys. Rev. D **87**, 053017 (2013)

[20] M. E. Luke, and A. V. Manohar, Phys. Lett. B **286**, 348 (1992).

[21] It is an observable in the low energy limit of the Compton scattering: D. Moreno, and A. Pineda, Phys. Rev. D **97** 016012 (2018); **98** 059902(E) (2018)

Size running $\tilde{D}_d^{(2)}$

To visualize the relative importance of the NLO/NLL corrections compared with the LO/LL terms we evaluate them:

B_c $(n_f = 3)$	$\nu = 1.1$ GeV
LO	1.09
LL (SL)	2.25 (1.70)
NLO	0.07
NLL ultrasoft (SL)	-0.18 (-0.04)
NLL soft (SL)	-0.04 (-0.02)
NLL new soft (SL)	-0.09 (-0.07)
NLL potential (SL)	0.63 (0.29)

Table: LO, NLO, LL, NLL and single log (SL) contributions to $\tilde{D}_d^{(2)}$ for the B_c system $(\nu_h = 2m_r = 2m_b m_c/(m_b + m_c))$ for $\nu = 1.1$ GeV in the case of $n_f = 3$.

Size running $\tilde{D}_d^{(2)}$

- The NLO corrections are small compared to the LO results, as expected.
- The NLL contribution is small compared to the LL one, as expected.
- The soft running is comparable to the ultrasoft running.
- The potential running is definitely more important than the soft and ultrasoft running.
- The resummation of large logarithms happens to be very important.

N^3LL heavy quarkonium mass

The spectrum at N^3LO was obtained

- For the ground state A. A. Penin, and M. Steinhauser, Phys. Lett. B **538**, 335 (2002).
- For S-wave states A. A. Penin, V. A. Smirnov, and M. Steinhauser, Nucl. Phys. **B716**, 303 (2005) and M. Beneke, Y. Kiyo, and K. Schuller, Nucl. Phys. **B714**, 67 (2005).
- For general quantum numbers but for the equal mass case Y. Kiyo, and Y. Sumino, Phys. Lett. B **730**, 76 (2014) and Y. Kiyo, and Y. Sumino, Nucl. Phys. **B889**, 156 (2014).
- For the unequal mass case C. Peset, A. Pineda, and M. Stahlhofen, J. High Energy Phys. 05, (2016) 017).
- The full result can be found in C. Peset, A. Pineda, and M. Stahlhofen, J. High Energy Phys. 05, (2016) 017 and in a different spin basis in C. Peset, A. Pineda, and J. Segovia, Phys. Rev. D **98**, 094003 (2018).

N^{3}LL heavy quarkonium mass

And at N^{3}LL

- For $l \neq 0$ C. Peset, A. Pineda, and J. Segovia, Phys. Rev. D **98**, 094003 (2018).

- for $l = 0$, $s = 1$ B. A. Kniehl, A. A. Penin, A. Pineda, V. A. Smirnov, and M. Steinhauser, Phys. Rev. Lett. **92**, 242001 (2004); **104**, 199901(E) (2010) and A. A. Penin, A. Pineda, V. A. Smirnov, and M. Steinhauser, Phys. Lett. B **593**, 124 (2004); **677**, 343(E) (2009) .

N^{3}LL heavy quarkonium mass

The purely N^{3}LL energy shift $\delta E_{nl,\mathrm{RG}}\Big|_{\mathrm{N^3LL}}$ generated by $\tilde{D}_d^{(2)}$ reads[22]

$$
\begin{aligned}
\delta E^{\mathrm{new}}_{nl,\mathrm{RG}}\Big|_{\mathrm{N^3LL}} \quad = \quad & \frac{1}{m_1 m_2}\pi C_F[\delta\tilde{D}_d^{(2)\,\mathrm{NLL}}(\nu_h,\nu) - \delta\tilde{D}_d^{(2)\,\mathrm{NLL}}(\nu,\nu)]\frac{(m_r C_F\alpha)^3}{\pi n^3}\delta_{l0} \\
& +2\frac{1}{m_1 m_2}\pi C_F[\tilde{D}_d^{(2)\,\mathrm{LL}}(\nu_h,\nu) - \tilde{D}_d^{(2)\,\mathrm{LL}}(\nu,\nu)]\left[-\frac{\alpha}{4\pi}\right]\frac{(m_r C_F\alpha)^3}{\pi n^3}\delta_{l0} \\
& \times\left\{2\beta_0\left[\frac{1}{2}+\frac{\pi^2 n}{6} - n\Sigma_2^{(k)}(n,0) - \frac{3}{2}\ln\left(\frac{na\nu}{2}\right) - \frac{3}{2}S_1(n)\right] - \frac{3}{2}a_1\right\} \\
& +\frac{\pi C_F}{m_1 m_2}\left[-\frac{1}{4\pi}\right]\frac{2(m_r C_F\alpha)^3}{n^3}\left(\ln\frac{na\nu}{2} - S_1(n) - \frac{n-1}{2n}\right)2\delta_{l0} \\
& \times\left[\left(k\frac{d}{dk}\tilde{D}_d^{(2)}\right)\Bigg|_{k=\nu}^{\mathrm{LL}}(\nu_h;\nu) - \left(k\frac{d}{dk}\tilde{D}_d^{(2)}\right)\Bigg|_{k=\nu}^{\mathrm{LL}}(\nu;\nu)\right], \qquad (38)
\end{aligned}
$$

where $\delta\tilde{D}_d^{(2)\,\mathrm{NLL}}$ is defined in Eq. (12). By adding $\delta E^{\mathrm{new}}_{nl,\mathrm{RG}}\Big|_{\mathrm{N^3LL}}$ to the already known contributions one obtains the complete N^{3}LL heavy quarkonium spectrum.

[22] Missing definitions can be found in C. Peset, A. Pineda, and J. Segovia, Phys. Rev. D **98**, 094003 (2018).

Conclusions

- We have computed the SI $\mathcal{O}(\alpha^2/m^3)$ and $\mathcal{O}(\alpha/m^4)$ potentials in the Coulomb gauge.
- We have computed the divergent part of the $\mathcal{O}(\alpha^3/m^2)$ SI delta-like potential proportional to c_F^2, $\bar{c}_1^{hl}$ in a general covariant gauge (proportional to c_k^2, d_{ss} and d_{vs} missing).
- We have quantified the mixing between the α^3/m^2 and the α^2/m^3 potentials proportional to c_F^2, which takes place when using the full EOMs in energy dependent potentials.

Conclusions

- We have computed and solved the NLL soft (partially) and potential RGEs of the Wilson coefficient $\tilde{D}_d^{(2)}$, associated to the SI delta-like potential.

- The missing terms to obtain the full result are:
  - The NLL running of $\bar{c}_1^{hl}$, whose associated missing contribution to the spectrum is of $\mathcal{O}(T_f n_f m\alpha^6 \ln\alpha)$, which is expected to be quite small.
  - The piece of the soft running proportional to c_k^2, d_{ss} and d_{vs}. This contribution is estimated to be smaller compared to the potential running, since the soft running is π^2 suppressed with respect to it.

- We have made an important step towards the determination of the S-wave ($l = 0$) spin-average (SI) heavy quarkonium spectrum with N^{3}LL accuracy, and therefore, of the full N^{3}LL spectrum.

Conclusions

- We remark that significant parts of the computations we have carried out are necessary building blocks for a future evaluation of the N^4LO ($m\alpha^6$) heavy quarkonium spectrum.

- The NLL running of $\tilde{D}_d^{(2)}$ is also one of the missing blocks to obtain the complete N^2LL expression of the Wilson coefficient of the electromagnetic current.
  This is indeed what is needed to achieve N^2LL precision for non-relativistic sum rules and the t-$\bar{t}$ production near threshold.

Questions

Introduction

We work in the $\overline{\rm MS}$ renormalization scheme, where the bare and renormalized couplings are related by $(D = 4 + 2\epsilon)$

$$g_B^2 = g^2 \left[1 + \frac{g^2 \bar{\nu}^{2\epsilon}}{(4\pi)^2} \beta_0 \frac{1}{\epsilon} + \left(\frac{g^2 \bar{\nu}^{2\epsilon}}{(4\pi)^2} \right)^2 \left[\beta_0^2 \frac{1}{\epsilon^2} + \beta_1 \frac{1}{\epsilon} \right] + \mathcal{O}(g^6) \right], \qquad (39)$$

$$\bar{\nu}^{2\epsilon} = \nu^{2\epsilon} \left(\frac{e^{\gamma_E}}{4\pi} \right)^{\epsilon}, \qquad (40)$$

where

$$\begin{aligned} \beta_0 &= \frac{11}{3} C_A - \frac{4}{3} T_F n_f \,, \\ \beta_1 &= \frac{34}{3} C_A^2 - \frac{20}{3} C_A T n_f - 4 C_F T n_f \,. \end{aligned} \qquad (41)$$

being n_f the number of dynamical (active) quarks and $\alpha = g^2 \nu^{2\epsilon}/(4\pi)$.

Introduction

The running of α is governed by the β function defined through

$$\frac{1}{2}\nu\frac{\mathrm{d}}{\mathrm{d}\nu}\frac{\alpha}{\pi} = \beta(\alpha) = -\frac{\alpha}{\pi}\left\{\beta_0\frac{\alpha}{4\pi} + \beta_1\left(\frac{\alpha}{4\pi}\right)^2 + \cdots\right\}. \tag{42}$$

Finally, let us define the following useful quantity

$$z \equiv \left(\frac{\alpha(\nu)}{\alpha(\nu_h)}\right)^{\frac{1}{\beta_0}} \simeq 1 - \frac{1}{2\pi}\alpha(\nu_h)\ln\left(\frac{\nu}{\nu_h}\right). \tag{43}$$

pNRQCD Lagrangian

We adopt the color normalization

$$\mathrm{S} = S\,\mathbf{1}_c/\sqrt{N_c}\,, \qquad \mathrm{O} = O^a \mathrm{T}^a/\sqrt{T_F}\,, \tag{44}$$

for the singlet $S(\mathbf{r}, \mathbf{R}, t)$ and the octet $O^a(\mathbf{r}, \mathbf{R}, t)$ fields.

$iD_0\mathrm{O} \equiv i\partial_0\mathrm{O} - g[A_0(\mathbf{R}, t), \mathrm{O}]$, $\mathbf{P_R} = -i\boldsymbol{\nabla}_\mathbf{R}$ (singlet), $\mathbf{P_R} = -i\mathbf{D_R}$ (octet), $\mathbf{p} = -i\boldsymbol{\nabla}_\mathbf{r}$, and

$$m_r = \frac{m_1 m_2}{m_1 + m_2}\,, \qquad M = m_1 + m_2 \tag{45}$$

r: quark-antiquark distance vector.
R: center-of-mass position of the quark-antiquark system.
t: time.
m_r, M are the reduced and the total mass of the system.

pNRQCD Lagrangian

The initial matching condition at NLO, $\tilde{D}_d^{(2)\,\mathrm{NLO}}(\nu_h)$, is also known. In the Coulomb gauge matching scheme is

$$\begin{aligned}\tilde{D}_{d,\mathrm{CG}}^{(2)}(\nu_h) \quad = \quad & 2\alpha(\nu_h) + \frac{\alpha^2(\nu_h)}{4\pi}\left(\frac{62}{9}C_A + \frac{4}{3}C_F - \frac{32}{3}C_A \ln 2 - \frac{28}{9}T_F n_f\right. \\ & \left. + \left(\frac{m_1}{m_2} + \frac{m_2}{m_1}\right)\left[-\frac{10}{9}T_F n_f + \left(\frac{61}{18} - \frac{16}{3}\ln 2\right) C_A\right]\right) \\ & + \frac{1}{\pi C_F}\left(d_{ss}(\nu_h) + C_F \bar{d}_{vs}(\nu_h)\right) . \qquad (46)\end{aligned}$$

The NRQCD Wilson coefficients c_D, d_{ss} and d_{vs} are known at one-loop order[23]. The numerical values of $\tilde{D}_d^{(2)\,\mathrm{NLO}}(\nu_h)$ are

- For B_c, 0.05, 0.07 and 0.14 for n_f=4, 3, and 0 (1.09 at LO).
- For bottomonium, 0.04, 0.05 and 0.08 for n_f=4, 3, and 0 (0.65 at LO).
- For charmonium, 0.11, 0.13 and 0.21 for n_f=4, 3, and 0 (1.05 at LO).

These corrections are small compared to the LO results.

[23] A. V. Manohar, Phys. Rev. D **56**, 230 (1997); A. Pineda, and J. Soto, Phys. Rev. D **58**, 114011 (1998).

Plots running $\tilde{D}_d^{(2)}$

In order to visualize the relative importance of the NLL corrections compared with the LL term, we plot them from $\nu = \nu_h$ to $\nu = 1$ GeV.

For reference, in this and later figures we use the following numerical values for the heavy quark masses and $\alpha(\nu_h)$:

- $m_b = 4.73$ GeV,
- $\alpha(m_b) = 0.216547$
- $m_c = 1.5$ GeV
- $\alpha(m_c) = 0.348536$
- $\alpha(2m_b m_c/(m_b + m_c)) = 0.290758$

And $\nu_h = m_b$ for bottomonium, $\nu_h = m_c$ for charmonium, and $\nu_h = 2m_r = 2m_b m_c/(m_b + m_c)$ for the B_c system.

Plots running $\tilde{D}_d^{(2)}$

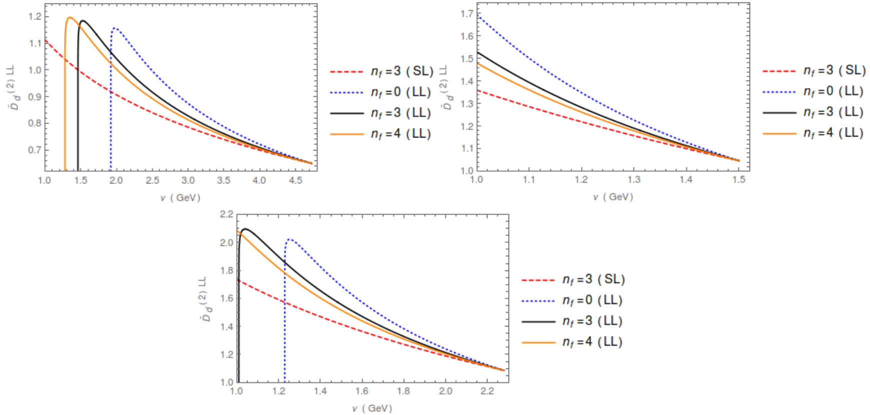

Figure: Plot of the LL running of $\tilde{D}_d^{(2)}$ in the off-shell (Coulomb/Feynman) matching scheme for different values of n_f (0,3,4) and in the SL approximation (only with $n_f = 3$). **Left:** Plot for bottomonium with $\nu_h = m_b$. **Right:** Plot for charmonium with $\nu_h = m_c$. **Center:** Plot for B_c with $\nu_h = 2m_b m_c/(m_b + m_c)$.

Plots running $\tilde{D}_d^{(2)}$

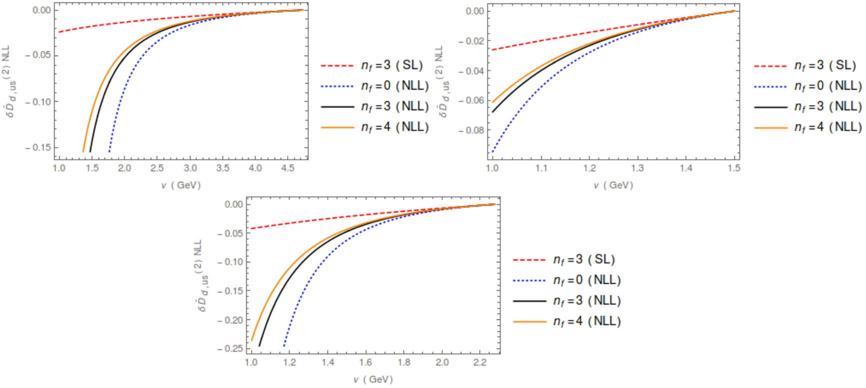

Figure: NLL ultrasoft running $\delta\tilde{D}_{d,us}^{(2)\,\mathrm{NLL}}$ in the off-shell (Coulomb/Feynman) matching scheme for different values of n_f (0,3,4) and in the SL approximation (only with $n_f = 3$). **Left:** Plot for bottomonium with $\nu_h = m_b$. **Right:** Plot for charmonium with $\nu_h = m_c$. **Center:** Plot for B_c with $\nu_h = 2m_b m_c/(m_b + m_c)$.

Plots running $\tilde{D}_d^{(2)}$

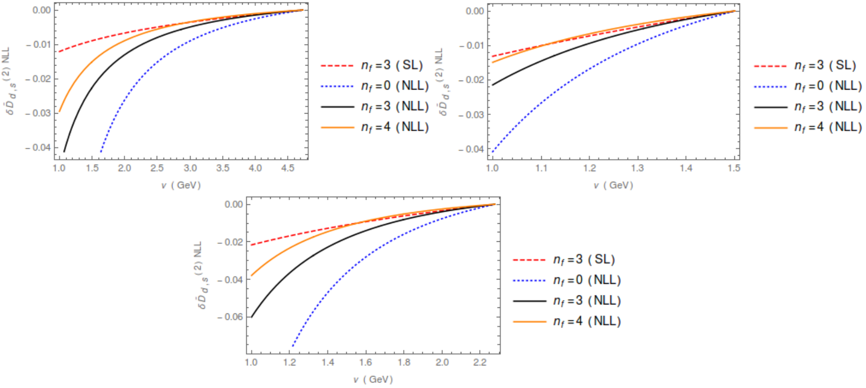

Figure: Plot of the NLL soft running $\delta\tilde{D}_{d,s}^{(2)\,\mathrm{NLL}}$ for different values of n_f (0,3,4) and in the SL approximation (only with $n_f = 3$). **Left:** Plot for bottomonium with $\nu_h = m_b$. **Right:** Plot for charmonium with $\nu_h = m_c$. **Centered:** Plot for B_c with $\nu_h = 2m_bm_c/(m_b + m_c)$.

Plots running $\tilde{D}_d^{(2)}$

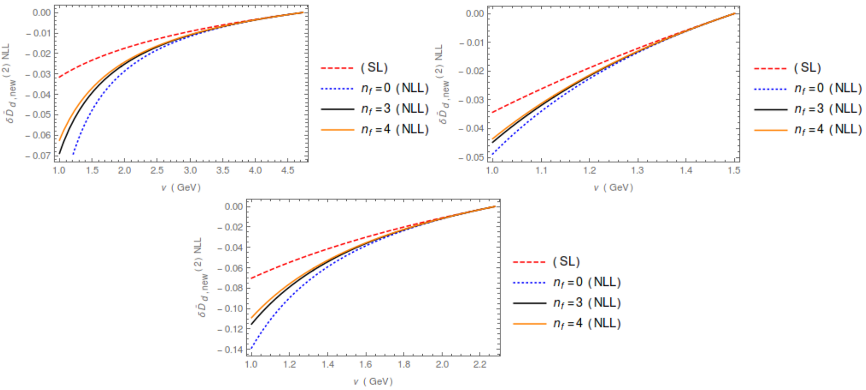

Figure: Plot of the extra contribution to the NLL soft running, $\delta\tilde{D}_{d,s}^{(2)\,\mathrm{NLL}}$, due to Eq. (35), for different values of n_f (0,3,4) and in the SL approximation (only with $n_f=3$). **Left:** Plot for bottomonium with $\nu_h=m_b$. **Right:** Plot for charmonium with $\nu_h=m_c$. **Centered:** Plot for B_c with $\nu_h=2m_bm_c/(m_b+m_c)$.

Plots running $\tilde{D}_d^{(2)}$

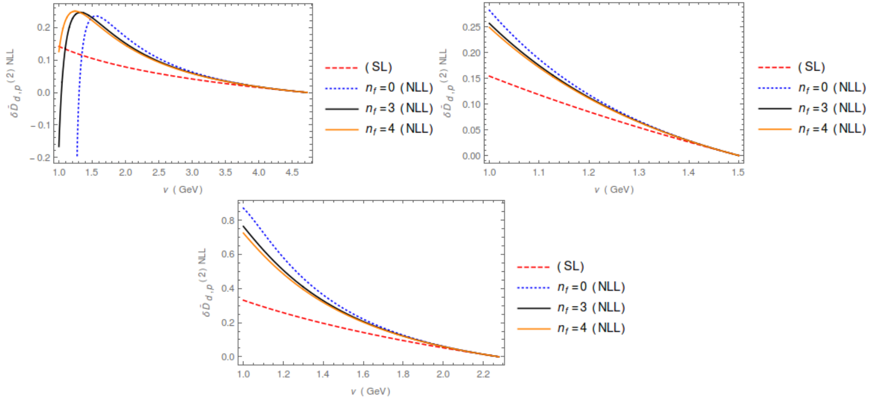

Figure: Plot of $\delta\tilde{D}_{d,p}^{(2)\mathrm{NLL}}$ for different values of n_f (0,3,4) and in the SL approximation (only with $n_f = 3$). **Left:** Plot for bottomonium with $\nu_h = m_b$. **Right:** Plot for charmonium with $\nu_h = m_c$. **Centered:** Plot for B_c with $\nu_h = 2m_b m_c/(m_b + m_c)$.

N^{3}LL heavy quarkonium mass

- The first three lines are generated by the term proportional to $\delta^{(3)}(\mathbf{r})$.
- The last two lines come from the Fourier tranform of the $\ln k$ term in $\tilde{D}_d^{(2)}$.

$$
\begin{aligned}
k\frac{d}{dk}\tilde{D}^{(2)}_{d,\mathrm{CG}}\Big|^{\mathrm{LL}}_{k=\nu}(\nu_h;\nu) \quad = \quad & -\beta_0\frac{\alpha^2}{\pi}+\frac{\alpha^2}{\pi}\left(2C_F-\frac{C_A}{2}\right)c_k^{(1)}c_k^{(2)} \\
& +\frac{\alpha^2}{\pi}\left[\frac{m_1}{m_2}\left(\frac{1}{3}T_f n_f \bar{c}_1^{hl(2)}-\frac{4}{3}(C_A+C_F)c_k^{(2)\,2}-\frac{5}{12}C_A c_F^{(2)\,2}\right)\right. \\
& \qquad \left.+\frac{m_2}{m_1}\left(\frac{1}{3}T_f n_f \bar{c}_1^{hl(1)}-\frac{4}{3}(C_A+C_F)c_k^{(1)\,2}-\frac{5}{12}C_A c_F^{(1)\,2}\right)\right] \\
& -\frac{(m_1+m_2)^2}{m_1 m_2}\frac{4}{3}\left(\frac{C_A}{2}-C_F\right)\frac{\alpha^2}{\pi}\left[\ln\left(\frac{\alpha(\nu)}{\alpha(\nu^2/\nu_h)}\right)+1\right].
\end{aligned}
\tag{47}
$$